Supplementary Figures

Supplementary Figure 1

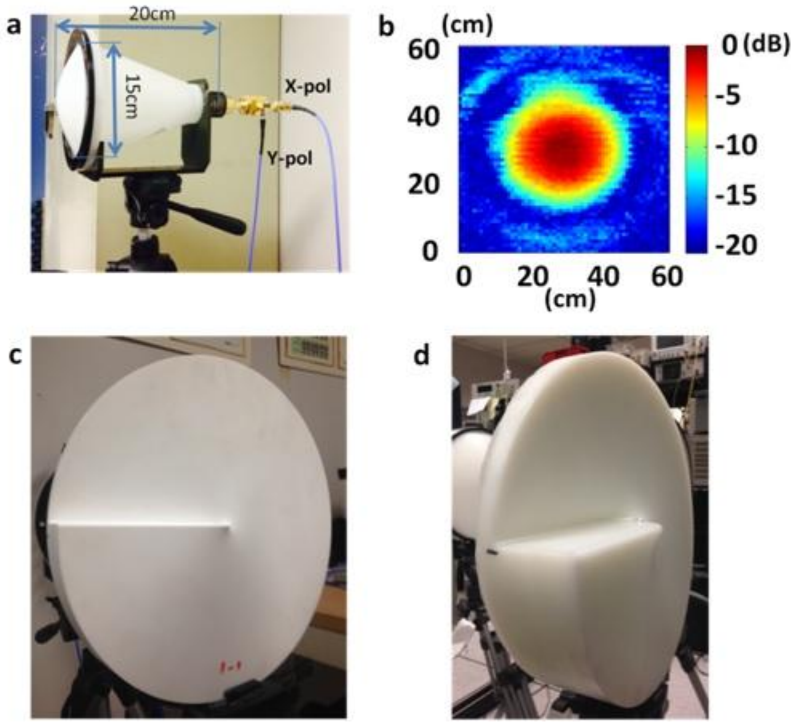

Supplementary Figure 1 | a, 50:50 dual-pol horn-lens antenna for generating Gaussian beams of X- and Y-polarisations. **b,** Intensity of the Gaussian beam emitted from the horn-lens antenna. **c** High-density polyethylene (HDPE) spiral phase plate (SPP) for transforming the input Gaussian beams into OAM beams of $\ell = \pm 1$. **d,** HDPE SPP for transforming the input Gaussian beams into OAM beams of $\ell = \pm 3$.

Supplementary Figure 2

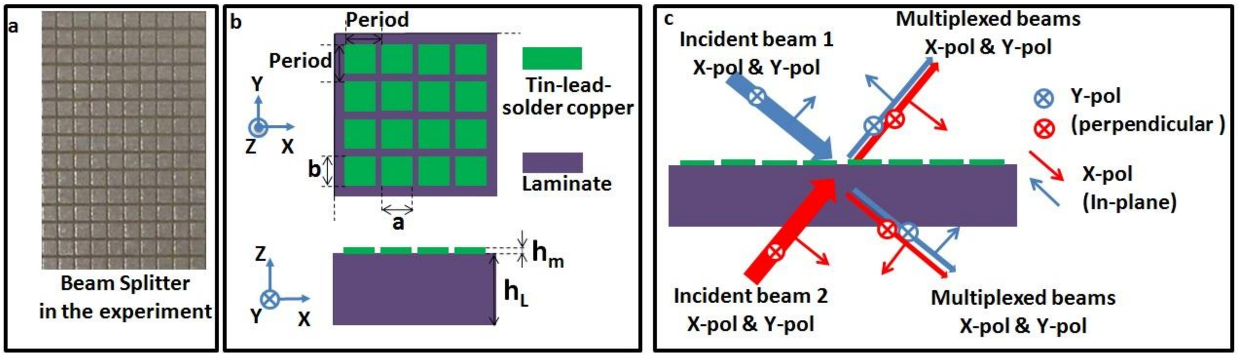

Supplementary Figure 2 | a, Beam splitter used to multiplex mm-wave OAM channels, fabricated via a standard printed circuit board process. **b,** Design of the mm-wave beam splitter of a two-dimensional metal array (tin-lead solder copper, array period of 0.254 mm) printed on an industry standard FR-4 laminate board. **c,** Illustration of the multiplexing mm-wave beams of two polarisations using a beam splitter.

Supplementary Figure 3

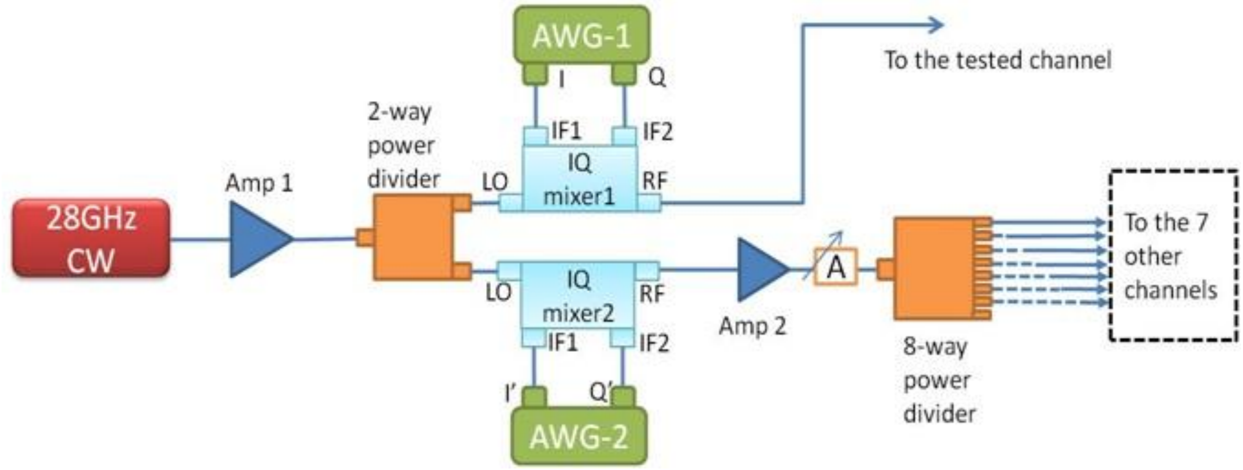

Supplementary Figure 3 | Diagram of the generation of 1Gbaud 16-QAM and QPSK signal (CW: continuous-wave, Amp: amplifier, AWG: arbitrary waveform generator, A: tunable attenuators). The signals generated by IQ mixer 1 and IQ mixer 2 are independent from each other. Attenuators and cables of different lengths are used after the eight-way power divider to decorrelate the signals on the other non-tested channels and generate eight channels of equal power.

Supplementary Figure 4

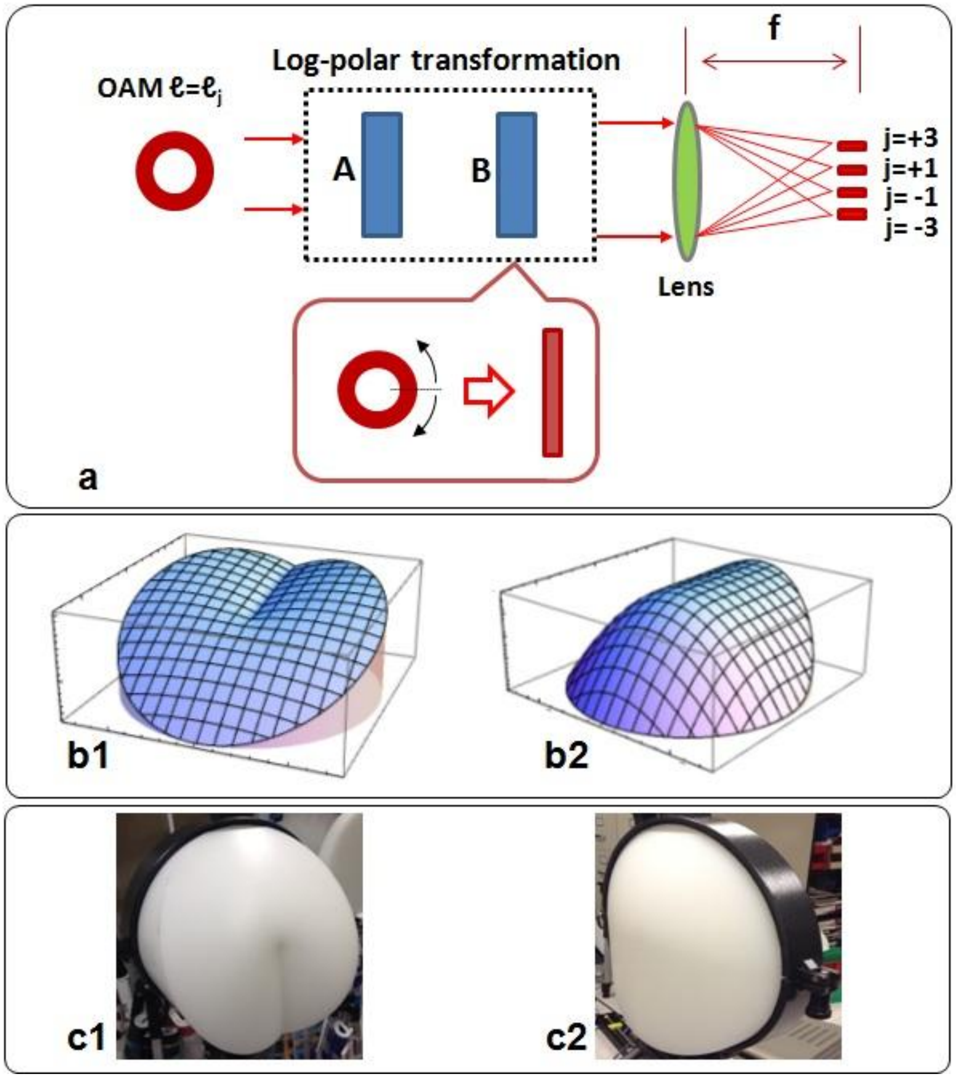

Supplementary Figure 4 | a, Concept of conversion of OAM states into transverse momentum states by using two refractive quasi-optical components. (a) Block diagram of a complete mode-sorting system, along with a positive lens at the output. **b1 and b2,** 3D models illustrating the height profiles of the two refractive components A and B, as shown in the block diagram. **c1 and c2**, Photos of the two refractive components used in the experiment.

Supplementary Notes

Supplementary Note 1: Generation of mm-wave OAM beams

We generated the mm-wave OAM beam by passing a Gaussian beam through a spiral phase plate (SPP). An orthomode transducer is used to multiplex two orthogonal polarisations, which were then fed to a horn-lens antenna. The horn-lens antenna generated an approximate Gaussian beam with two orthogonal polarisations and a beam waist of 15 cm at the horn exit aperture (see Supplementary Fig. 1a). Supplementary Figure 1b shows the intensity of the emitted Gaussian beam, as recorded by the probe antenna on a motorised two-dimensional stage. The SPPs for generating mm-wave OAM beams of $\ell = \pm1$ and $\ell = \pm3$ are shown in Supplementary Figs. 1c and 1d, respectively.

Supplementary Note 2: 50:50-ratio 28-GHz mm-wave beamsplitter

The beamsplitter used to multiplex the mm-wave OAM beams is a two-dimensional rectangular grid of reflective material supported by a dielectric substrate (see Supplementary Fig. 2a). The beam splitters were fabricated via a standard printed circuit board (PCB) process. The design of the beam splitter is shown in Supplementary Fig. 2b. The reflective material layer is tin-lead solder copper with a thickness of h_m=0.004 cm, and the dielectric substrate material is industry-standard FR-4 laminate. The laminate layer has a refractive index of 2.04~2.23 at 28GHz, and the thickness is h_L = 0.15 cm. The period of the grid in the X and Y directions is 0.254 cm, which is about one quarter of the wavelength at 28GHz. For a mm-wave beam incident at 45 degrees, only the zeroth-order reflected and transmitted beams exist, and there is no higher-order diffracted beam. To achieve 50% reflection and transmission for both the X and Y polarisation states at an incidence angle of 45 degrees, the side lengths of the metal square were designed to be a=0.85×0.254cm and b=0.8×0.254cm. The beam splitter design is based on finite-difference time-domain (FDTD) simulations[40].

Supplementary Note 3: Generation of 1-Gbaud/s 16-QAM and QPSK signal at 28-GHz carrier frequency

A block diagram of the generation of 1-Gbaud 16-QAM for each of the eight channels is shown in Supplementary Fig. 3. A 28-GHz continuous-wave (CW) signal was generated by a radio frequency oscillator and amplified by a 1-watt amplifier (Amp1). The amplified CW was split into two paths by a two-way power divider to serve as the LO inputs for two IQ mixers. Two arbitrary waveform generators were used to generate two independent pairs of I and Q waveforms of 1-Gbaud four-level amplitude-modulation signals and were connected to the IF ports of the two IQ mixers. The signals generated by the AWGs were pseudorandom binary sequences (PRBS) of length 2^{15}-1. At the outputs of the two IQ mixers, we had two independent 1-Gbaud 16-QAM data streams at a carrier frequency of 28GHz. The data stream from I-Q mixer 1 was connected to one OAM channel, which is demultiplexed and detected for BER measurements. In order to generate source signals for the remaining seven OAM channels, the independent data stream from I-Q mixer 2 is amplified and split into eight paths using an eight-way power divider. The seven outputs from the eight-way power divider were decorrelated by using cables of different lengths and were connected to seven OAM channels, while the eighth output remained unused. Due to time delays, different symbols were applied to each of the interfering channels at different points in time. Attenuators were used before and after the eight-way power divider so that all of the eight channels would have the same power before entering the antennas. This configuration ensured that the data on a tested channel were independent of data on other non-tested interfering channels, whose data streams were mutually decorrelated. In order to measure the crosstalk and BER for a specific OAM channel, we connected the 16-QAM signal generated from IQ mixer 1 to the tested channel and reconfigured the attenuators and cables to have equal power for all eight channels.

For the 1-Gbaud QPSK signal generation in the four-OAM-channel experiment, the procedure described above is followed, except that each AWG generated independent pairs of I and Q waveforms of the 1-Gbaud two-level amplitude-modulation signals. The output from I-Q mixer 1 is used as one of the OAM channels, while only three outputs of the eight-way power divider were used for the remaining three channels.

Supplementary Note 4: Detection of 1-Gbaud/s 16-QAM and QPSK signal at 28-GHz carrier frequency

For signal detection, we used an 80-GSample/s real-time oscilloscope, whose real time analogue bandwidth of 32GHz was wide enough to faithfully capture the mm-wave waveform of 1-Gbaud, 16-QAM or QPSK signals at a 28-GHz carrier frequency. A pre-amplifier is used for the OAM mode demultiplexer experiment after the received probe antenna because the probe antenna aperture is too small (diameter = 0.7 cm) to receive enough power for detection. For the part of the experiment in which the OAM channels were sequentially demultiplexed, the 15-cm-diameter horn-lensed antenna was used to receive the signal, without the use of any pre-amplifier. A variable attenuator is placed before the real-time oscilloscope to vary the signal-to-noise ratio (SNR). A total of 2×10^6 points were sampled in real time, which corresponds to 2×10^5 bits for the 1-Gbaud 16-QAM signal and 1×10^5 bits for the 1-Gbaud QPSK signal. The sampled points were processed offline to recover the 16-QAM or QPSK signal and to calculate the BER. The offline processing procedures included the following sequential steps: carrier frequency recovery, carrier phase estimation, down-conversion and low-pass filtering. The recorded sequence is first fast-Fourier transformed (FFT) for the carrier frequency estimation. Consequently, the carrier phase that minimised the error-vector magnitude (EVM) of the demodulated signal is found. The procedure is followed by digital frequency down-converting the I and Q channels. The down-converted signal is then filtered with a rectangular-shaped low-pass filter and converted to the time domain using inverse fast-Fourier transformation (IFFT). The binary data decision and error bit counting then produce the measured BER.

Supplementary Note 5: Design of mm-wave OAM mode demultiplexer

The schematic setup of the OAM mode demultiplexer (see Supplementary Fig. 4a) is essentially comprised of two refractive elements and a positive lens. The principle of the OAM mode demultiplexer is to first introduce a spatially-dependent deviation to the rays in the incoming ray bundle such that the rays arrive at the required position upon propagation to the second element. The role of the second element is to ensure that relative phase is preserved. The positive lens placed after the second element transforms the power of each input OAM mode into a fixed spatial location in the output plane that depends on ℓ. Three-dimensional models of the two components are shown in Supplementary Fig. 4b. The real components used in the experiment are fabricated by using HDPE through CNC milling methods and are shown in Supplementary Fig. 4c. The performance of the two refractive components in terms of demultiplexing the mm-wave OAM modes is tested by propagating OAM modes through the two OAM mode demultiplexer components, which were properly placed along the direction of propagation. To determine the spatial intensity profile after the positive lens, an antenna is placed on a two-dimensional motorised translation stage. The power is measured at discrete spatial positions, with a spacing of 1 cm between positions. Four different OAM modes with $\ell = \pm 1, \pm 3$ are tested, and the cross-sections of the spatial variations in the intensities of each mode are measured. It can be seen in Supplementary Fig. 4 that given a change in the input OAM mode, there is a lateral shift of the peak position of the focused spot. The transverse position of the spot changes as a function of ℓ and can be predicted to shift by $\Delta x_\ell = \frac{\lambda f}{d} \ell$, where λ is the wavelength, *f* is the focal length of the positive lens and *d* is the width of the transformed beam.

The crosstalk of the OAM channels is characterised by transmitting four multiplexed OAM beams ($\ell = +1$ and $\ell = -1$, each of which has two independent linear polarisations) through the link using a CW signal at 28 GHz. The crosstalk between these channels is measured by testing each channel independently and by normalising the crosstalk with respect to the total received power. For each OAM channel carrying a 1-Gbaud QPSK channel, the BER is measured for three different cases: 1) when no crosstalk from other channels is present, 2) when there is crosstalk from the other OAM channel with the same polarisation and 3) when there is crosstalk from the other OAM channels on both polarisations.